A new cross contamination aware routing method with intelligent path exploration in Digital Microfluidic Biochips

Conference Paper · March 2013

CITATIONS
0

READS
41

5 authors, including:

Pampa Howladar
Indian Institute of Engineering Science and Tec…
5 PUBLICATIONS **0** CITATIONS
SEE PROFILE

Pranab Roy
Indian Institute of Engineering Science and Tec…
46 PUBLICATIONS **71** CITATIONS
SEE PROFILE

Hafizur Rahaman
Indian Institute of Engineering Science and Tec…
339 PUBLICATIONS **871** CITATIONS
SEE PROFILE

Parthasarathi Dasgupta
Indian Institute of Management Calcutta
92 PUBLICATIONS **238** CITATIONS
SEE PROFILE

A new cross contamination aware routing method with intelligent path exploration in Digital Microfluidic Biochips

Pranab Roy[1], Pampa Howladar[2],Rupam Bhattacharjee[3], Hafizur Rahaman[4]
[1,2,3,4] School of VLSI Technology
Bengal Engineering and Science University, Shibpur, INDIA
Email – [1]ronmarine14@yahoo.co.in , [2]p.howladar@gmail.com , [3]th_rup@yahoo.co.in , [4]rahaman_h@yahoo.co.in

Parthasarathi Dasgupta[5]
[5]Indian Institute of management, Calcutta, INDIA
Email – [5]partha@iimcal.ac.in

Abstract— Digital microfluidic systems in recent years have been developed as an alternative platform for execution of multiple conventional laboratory methods simultaneously on a single planar 2D array of electrodes targeted for biochemical analysis and biomedical applications. Due to its discrete nature droplets can be manipulated through multiple reconfigurable paths derived by preprogrammed electrode actuation sequences through this planar array known as digital microfluidic biochip system. Cross contamination between heterogeneous samples turns out to be a major issue concerned with transportation of droplets and correctness of the detection results for the bioassay protocols –which is highly significant for clinical diagnostics and toxicity monitoring applications. In this paper we have proposed an intelligent route path exploration technique that attempts partially or completely to avoid the number of cross contamination depending on the fluidic constraints employed during routing .The path is further refined using intelligent detour by identifying zones of friction between two adjacent route paths that optimizes the overall route time by reducing the overall time for stalling while routing –as well as further optimization of resources to be utilized. The simulation is carried out on test benches of benchmark suite I and benchmark suite III. The results show improvement in overall as well as average route time and major reduction in the number of crossovers.

Keywords- digital microfluidics, Cross contamination, routing, detour, algorithm, resource utilization.

I. INTRODUCTION

The miniaturization, integration, and parallelization of common laboratory processes in lab-on-a-chip systems have potentially transformed conventional laboratory procedures, (usually cumbersome and expensive) into low cost and synthesizable series of operations that involves multiple chemical manipulations on a single monolithic platform. The major advantage of such devices lies in higher sensitivity, better accuracy, lower cost as well as portability and higher levels of system integration. The miniaturization incorporated in these devices leads to shorter detection times, high throughput and reduction on energy as well as reagents consumption in biological experiments.

A popular class of commercially available biochips are based on continuous fluid flow being controlled by micropumps, microvalves, electrokinetics, or electroosmosis. In late 1990s an alternative class of lab-on-chip system which is capable of manipulating discrete droplets in volumes of nanolitres has been emerged. These new class of devices termed as Digital microfluidic biochip(DMFB) performs the process of droplets manipulation through different mechanisms, viz. electrowetting [1-2], dielectrophoresis [3], thermo capillary transport [4], and surface acoustic wave transport [5]. In the digital microfluidic architecture the basic liquid unit volume is fixed by the geometry of the system (fluid quantization), whereas volumetric flow rate is determined by the rate and the number of droplet transport. Compared to continuous flow-based techniques, digital microfluidics offers the advantage of individual sample addressing, reagent isolation, and compatibility with array-based techniques used for biochemical and biomedical application [1, 6].

Electro wetting on dielectric (ewod) is currently used as one of the best actuation methods for droplet manipulation in digital microfluidic systems [7]. it has emerged as an useful tool for biomedical applications such as polymer chain reaction (pcr) [8], enzyme assays [9], proteomics [10], dna hybridization and soft printing [11]. Generally, the mechanism of electro wetting phenomenon is based on control of surface tension of a liquid-solid interface by applying electrical potential at the interface. At the nanolitre scale, forces of interfacial tension between three phases dominate a droplet's hydrodynamic behavior. These include a force on the interface between the droplet and the ambient fluid, and a force acting on the triphase contact line where the droplet, the ambient fluid, and the solid meet. Electrocapillarity, that provides the distribution of free charges on the interfaces between different phases, modulates interfacial tension forces to manipulate droplets [13]. Thereby whenever a droplet is kept in contact with a solid electrode, a wetting force can arise upon application of an electric field through these electrodes. This wetting force acting on the triphase contact line can be altered by applying varied electrical potential to the droplet through the electrodes [12]. Hence by application of a programmed sequence of electric potential at consecutive electrodes a strength disparity of this wetting force is created and this results in movement of droplets from one electrode contact to an adjacent one.

This manipulation of discrete droplets allows to classify the microfluidic operations into a set of basic operations namely mixing, merging, splitting, storage and transportation. Hence the use of unit volumes of droplets can be accomplished in a 2D planar array of electrodes configured for an Electrowetting on dielectric system. The microfluidic array contains a set of basic cells that is made up of two parallel glass plates (Figure 1). The bottom plate contains a patterned array of individually controllable electrodes, and the top plate is coated with a continuous ground electrode. The filler medium, such as silicone oil, along with the sample droplet is sandwiched between the two plates. By assigning time-varying voltage values to turn on/off the electrodes on the digital microfluidic biochip, the interfacial tension of the droplets are modulated- resulting in their transportation around the entire 2-D array and execution of fundamental microfluidic operations for different bioassays. The operations performed by actuating control voltages through the electrodes are also called *reconfigurable* operations because of their flexibility in location and in execution time. Such reconfigurable operation can be carried out at any prescheduled place within the 2-D plane. Hence the DMFS offers a platform that provides the advantage of dynamic reconfigurability and software based control for multifunctional biochips.

Two major resource components involved in performing fundamental operations in a DMFB are the Mixers and Storage units consisting of electrodes. Mixers are used to perform mixing and splitting operations, whereas storage units are used for storage of droplets generated for subsequent mixings. Transportation paths are used to move droplets among different components (e.g., mixers and storage units) within the 2D array. In addition the array may contain cells that can perform specialized operations, such as heating or optical sensing.Hence transportation of droplets in DMFBs figures out to be a major step regarding the overall operation and results obtained in digital microfluidic systems. The dynamic reconfigurability inherent in DMFBs allows for sharing of cells by multiple droplets routes in a time multiplexed manner. If the microfluidic system is designed for execution of multiple bioassay

978-1-4673-6040-1/13/$31.00 ©2013 IEEE

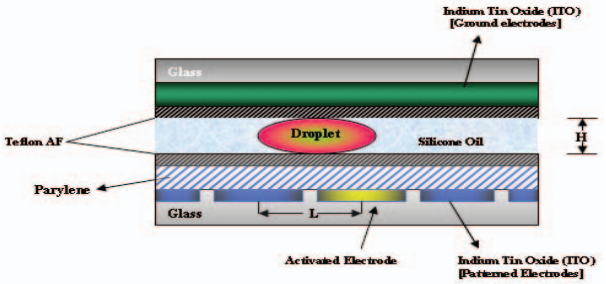

Figure 1 – Schematic diagram for droplet movement in a DMFB

protocols involving heterogeneous samples – this sharing phenomenon may result in a major problem termed as cross contamination. Such contaminations caused by bead retention and liquid residue between successive droplet routes of different droplet samples may result in inevitable erroneous reaction that produces incorrect detection outcomes. In addition excessive and prolonged contamination may result in breakdown of the electrodes as well as electrode short problems. This finally generates physical defects and produce incorrect behaviours in the electrical domain [15].

Thereby it becomes necessary to design algorithms that plan the droplets to be routed in disjoint manner. With further increase in the levels of integration as well as degree of scaling – finding of disjoint route within a predetermined layout becomes increasingly difficult. This in turn reduces the availability of the number of spare cells – that can be used to replace the defective primary cells (while rerouting to avoid faulty cells) - hence compromising with the defect tolerance for the given bioassay.

In this paper we have proposed a cross contamination aware routing method that involves intelligent exploration between suitable route path for each sample droplets – that not only minimizes or eliminates the number of cross contaminations but also with further refinement in terms of detour or optimized alteration - the overall route time as well as cell utilization can be optimized. The organization of the rest of the paper is as follows .Section II discusses the related works regarding droplet routing and cross contamination issues. Section III formulates the droplet routing problems and the constraints involving cross contamination. Section IV states the motivation and the contribution of our work. Section V elaborates the designed algorithm with an illustrative example stated in Section VI. In Section VII the experimental simulation results are displayed together with the corresponding comparisons with results obtained from contemporary methods. Finally Section VIII states the concluding remarks and the future scopes for further enhancement.

II. RELATED WORKS

The issue of simultaneous droplet routing within a DMFB involves major objectives namely the optimization of the latest arrival time of all droplets from source to target, as well as the overall transport time for all the droplets and optimization of the cell (electrode) utilization in the process. Different algorithms have been proposed in an attempt to resolve the droplet routing issues with necessary optimization while maintaining the requisite constraints to achieve the objectives stated above. A direct addressing method is used in [16] where the droplet routing problem is mapped into a graph clique model. An integer linear programming (ILP) formulation based on direct addressing mode is reported in [17]. The movement of droplets at each time step is determined by solving an ILP. A 'droplet movement cost' is used as a heuristic to evaluate congestion when solving the ILP. In [18], dynamic reconfigurability of the microfluidic array is exploited during run-time. A high performance droplet routing algorithm using grid-based representation is reported in [19]. A partition-based algorithm for pin-constraint based design is proposed in [20]. Another fast routability and performance-driven droplet router for DMFBs has been proposed in [21]. A recent work based on Soukup's routing algorithm [22] for concurrent path allocation to multiple droplets appears in [23].Finally a pre-placed module based routing method is proposed in [24] which displays much improved results for cross referencing Biochips.

The issue of cross contamination was initially addressed in [25]and [29].In [25] wash droplets are introduced – to overcome the problem of contamination at any particular site and specific strategies are designed (baseline1 and baseline2) to synchronize the wash droplet operation with functional droplet route operations. [15] attempted to handle the issue of cross contamination by first using k-shortest path routing techniques to minimize the routing complexities as well as cell utilization and thereby reducing the number of contamination spots in the process. Then, to take advantage of multiple wash droplets, a minimum cost circulation algorithm (MCC) for optimal wash-droplet routing to simultaneously minimize the number of used cells and the cleaning time has been adopted. Moreover, a look-ahead prediction technique has been used to determine the contaminations between successive subproblems. It has been found that results obtained in[15] has been vastly improved as compared with [25]and [29]. To make the biochip feasible for practical applications, pin-count reduction poses another major design problem – which has been addressed with a pin count aware strategy (using a two staged ILP based method) integrating the contamination issues in [26]. In [28] a method has been proposed that utilized a graph based heuristics to select the best suitable path for routing using multiple alternative routes to avoid collision or violation of fluidic constraints. However the algorithm was focused only on collisions to minimize stalling resulting in substantial improvement in the route time. In [28] the cross contamination issues were not addressed – this renders the method to be suitable only for homogeneous sample applications.

In all of the above methods different routing strategies are prescribed for optimized contamination. Here we used a method to introduce intentional redundancy for estimating at least one alternative for each path with minimum deviation for each sample during virtual route estimation phase. We thereby attempted an intelligent exploration strategy to select iteratively most suitable minimum deviation paths among available alternatives to optimize cross contamination to a minimum or zero. An efficient trade off strategy has been adopted to avoid or minimize stalling using alternative deviation or detour to minimize the latest as well as average arrival time. Test benches from benchmark suite I and III has been used for implementation of the proposed strategy and the simulation results are displayed in section VII.

III. DROPLET ROUTING AND CROSS CONTAMINATION IN DMFB

The objective of droplet routing is to transmit all the droplets from their respective sources to targets within a 2D grid array while fulfilling all the constraints imposed for the transportation. An efficient routing schedule (virtual route) is often required to be developed to provide an optimal routing in terms of objectives such as latest arrival time and overall cell utilization. Droplet routing problem in *DMFB*s is typically modeled in terms of a 2D-grid (Figure 2). For each droplet, there exists a set of source grid locations, a set of target grid locations, and (optionally) a set of mixers. Each source-target combination is defined as a net. A 2-pin net has a single source and single target. A combination of two Sources, one Mixer and one Target forms a 3-pin net.

In cases of 3-pin nets, droplet merging is destined at predefined locations called mixers. Several microfluidic modules may be placed as per schedules for mixing, splitting, storage, dispensing and other operations within the array. These are considered as the *Hard Blockages*. In order to avoid conflicts between droplet routes and assay operations, a segregation region is defined around the functional region of each such microfluidic modules. Moreover, there are possibilities of intersection or overlapping of droplet routes during their concurrent routing in time-multiplexed manner. To avoid such undesirable behaviors following fluidic constraints are introduced.

Let d_i at (x^t_i, y^t_i) and d_j at (x^t_j, y^t_j) denote two independent droplets at any given timestamp t. Then, the following constraints, defined as Fluidic *Constraint*s are required to be satisfied for any time t while routing [27]:

Static constraint: $|x^t_i - x^t_j| > 1$ *or* $|y^t_i - y^t_j| > 1$

Dynamic constraint: $|x^{t+1}_i - x^t_j| > 1$
or, $|y^{t+1}_i - y^t_j| > 1$
or, $|x^{t+1}_j - x^t_i| > 1$ or $|y^{t+1}_j - y^t_i| > 1$

This implies that for any droplet at location **(x, y)**, the locations **(x+1, y), (x-1, y), (x, y+1), (x, y-1), (x+1, y+1), (x+1, y-1), (x-1, y-1)** and **(x-1, y+1)** are prohibited for any other droplet to enter at timestamps ***t*** and ***t+1*** in order to maintain these fluidic constraints. Hence, all the locations adjacent to **(x, y)** as stated above form a *Critical Zone* (Figure 2) for any droplet at **(x, y)** at timestamp ***t***. A predetermined time limit called the *Timing Constraint* defines the maximum allowed transportation time for a given set of droplets.

During this transportation process intersection between multiple routes may occur – causing a droplet arriving at the intersection location at a later clock cycle can be contaminated by the residue left behind by another droplet already crossing the said location at an earlier clock cycle. This phenomenon is termed as cross contamination and the locations shared by multiple droplets while routing are defined as cross contamination sites. Cross-contamination is undesirable during droplet routing since it leads to erroneous assay outcomes – as well as physical defects for prolonged operation. Figure 3 shows the instance of cross contamination at any given timestamp within a DMFB.

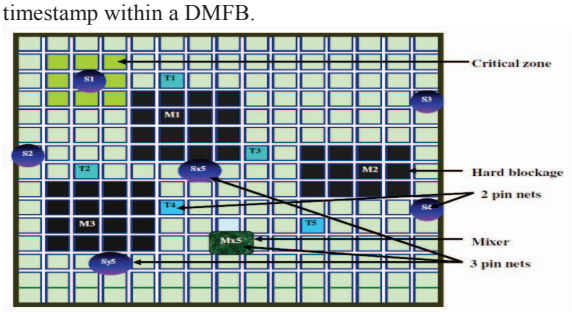

Figure 2: 2-pin and 3-pin nets in a 2D Grid Array; Critical zone for S1 is the **Green** shaded region. A hard Blockage is also illustrated.

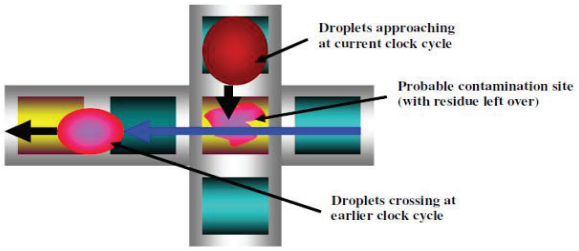

Figure 3: Instance of contamination within a DMFB while routing

IV. MOTIVATION AND OUR CONTRIBUTION

As evident from the earlier discussions cross contamination avoidance has turned out to be a major issue both in context of reliability of results as well as operation of the device. Few methods has already been proposed to tackle these issues as mentioned in section II. Initially the focus was at the estimated route tracks – by consciously allowing detour of droplets while routing to avoid cross over and thereby reducing the number of cross contamination locations. For 3 pin droplets different sources of the same net may be allowed to share the same path as mixing may not interfere with the accuracy of results in such cases. These types of cross over or sharing of cells are termed as allowable contamination. Hence it has been found that while optimized routing reduces the number of contamination – at the same time the two major objectives for routing has been compromised – by allowing an increase in latest arrival time as well as cell utilization in order to accommodate the intentional detour.

In this work we attempted to resolve these issues simultaneously to optimize the route performance in terms of overall route time together with reduction in the number of contaminations. The summary of the work is depicted below:

- For each net (if source and target are not in the same row or column) we have estimated two alternative Manhattan paths with minimum deviation in order to introduce intentional redundancy ignoring any modules coming in the way of theses routes as obstacles.
- Using a graph based heuristics we iteratively eliminated one alternate route while selecting the most suitable one in terms of contamination avoidance.
- Now we consider all those paths that cross through the modules and determine two alternate possible detours constituting again two alternatives.
- Again using a graph based heuristics we attempted to select the suitable deviation that again minimizes the additional contamination (if any- caused by these deviations) as well as the number of cells covered.
- Finally we define friction zones for all those parallel route path that covers certain neighbouring cells – thereby inviting possibility of stalling.
- On estimation of the time stamps at these neighbouring cells for the corresponding routes – if possible stalling is predicted we explored further possible detour that trades off with possible stalling in terms of reduction in overall route time that results in enhanced route performance.

V. THE PROPOSED METHOD

Here we start with a given layout comprised of a given number (n)of 2-pin and 3-pin nets.The objective is to determine n number of suitable route paths that results in C number of contaminations where minimum(number of contaminations) = C,alongwith latest arrival time T being the minimum as well as total cell covered E being optimum.

A. Proposed Algorithm

Input : A MxM 2D grid containing n number of samples comprising of x number of 2 pin and y number of 3 pin droplets.

Procedure :

Step 1 –Here each 3 pin net has been decomposed into three possible nets namely from source1 to mixer,source2 to mixer and mixer to target. each 2 pin net we assume one single net i.e. from source to target.

Hence for n number of samples possible nets $k = x + 3 * y$.

Step 2 – out of these k number of nets let p number of nets share the same rows or columns – thereby having only one estimated route path. For the (k-p) number of nets we estimate two alternate manhattan paths ignoring any passage through the modules termed as hard blockages.

Hence ,total number of estmated route paths $R = p + 2*(k-p)$.

Step 3 – We first draw a droplet intersection graph $G_D = (V_D , E_D)$ where $v \in V_D$ represents each droplet and $e(v_i , v_j) \in E_D$ exists if there are crossovers between paths of droplet v_i and v_j.each such edge e is assigned an weight w_{ij} representing total number of paths colliding between v_i and v_j .

Step 4 – Then we draw a path intersection graph $G_P = (V_P , E_P)$, where $v \in V_P$ represents each path and $e(v_x , v_y) \in E_P$ exists if there are crossovers between paths v_x and v_y. Each edge e has been assigned an weight w_{xy} representing number of cells contaminated during each crosover. There will be R number of vertices in G_P that represents total number of estimated paths(inclusive of intentional redundancy).

If the path represented by v_i crosses a module M_x attach v_i to a new block vertex M_x through a different color edge em_{ix}.

Step 5 – form a table T_{path} to map each vertex v_{x1} with its alternate v_{x2}9if any).otherwise keep the alternate column blank.

Step 6 – in Graph G_P arrange all the vertices in descending order of degrees and number them from 1 to R in the same order.

For i = 1 to R

For vertex $v_i \in V_P$ (if v_i exists and is not deleted already)

If $deg(v_i) > deg(alternate(v_i))$[if alternate of v_i exists in T_{path}]

Delete v_i with all the the corresponding edges incident on v_i.

If $deg(v_i) = deg(alternate(v_i))$[if alternate of v_i exists in T_{path}]

Compute weight(v_i) = W1= Σw_{xy} (summation of weights of all edges of incident on v_i)

Compute weight(alternate(v_i)) = W2 = Σw_{xy} (summation of weights of all edges of incident on alternate(v_i)).
If W1 >W2
Delete v_i with all the the corresponding edges incident on v_i.
Else if W2 >W1
Delete alternate(v_i) with all the the corresponding edges incident on alternate(v_i).
Else [for the case W1= W2 and deg(v_i) = deg(alternate(v_i))]
If either of v_i or alternate(v_i) has edge e_{mx} bound to module M_x
Delete the corresponding vertex and with all the edges incident on it (i.e. v_i or alternate(v_i) whichever applicable)
Next i.

Step 7 – Now draw the layout with remaining paths after deletion. There may still remain some redundant paths for certain nets.Now assume total S number of paths are left within the new layout after deletion.

Step 8 – Let there be L number of paths that passes through hard blockages .For each such path determine two possible deviations to bypass the corresponding blockages. Hence total number of paths available R = (S-L) + 2*L.

Step 9 – Again draw a path intersection graph from this remaining layout and repeat from Step 4 to Step 7 until all paths are addressed.

Step 10 – Out of these S number of remaining paths finally obtained – identify those paths that forms zones of friction. Zone of friction is defined as zones comprising of cells that constitute part of two neighbouring rows or columns - which has been utilized by two corresponding route paths.

Step 11 – in this final path intersection graph form a hyperpath connecting any two paths(vertices) that form each friction zones.
Each friction zone(hyperpath)conncts only two vertices v_x and v_y
For each friction zone (hyperpath)
If alternate(v_x) exists and does not belong to any other hyperpath
Delete v_x with all the the corresponding edges incident on v_x .
Else if alternate(v_y) exists and does not belong to any other hyperpath
Delete v_y with all the the corresponding edges incident on v_y .
Else if no alternate vertex exists for either v_x or v_y
Mark the zone as inevitable friction zone and explore a possible detour for either v_x or v_y whichever suitable and covers minimum number of additional cells with no contaminations.

Step 12 – in the final path intersection graph let the number of remaining vertices be V_{P1} and edges E_{P1}. These edges represent number of unavoidable crossovers and sum(weights of edges) W_{P1} represents the total number of unavoidable collisions.rearrange all vertices again in descending order of their degrees.

Step 13 –
For i = 1 to V_{P1}
If for v_i there exists an alternate(v_i)
Delete any one of these two with all the incident edges(if any) .
Next i.

Step 14 – Estimate the total number of crossovers and friction zones left over within the final path intersection graph. Draw the final layout and form the final droplet intersection graph as drawn in step 3.

Step 15 – Estimate the Manhattan distance D_i for each net. During concurrent routing of several droplets, there still remains a possibility of collision or overlap of paths between multiple droplets. In such a case, priorities are given in favour of the droplets with larger D_i. For 2-pin nets, each droplet is routed directly from its source to its target. For 3-pin (multi-pin) nets, routing from each of the sources S_x and S_y to the mixer (M) is done concurrently. This part of routing is referred to as the First Generation route. The largest arrival time T_{SM} between ($S_x \rightarrow M$) and ($S_y \rightarrow M$) is noted. The final mixed droplet from M is next routed to Target T. This is called the Second Generation route. For 2nd generation route, the timestamp starts from T_{SM} as determined earlier.

Step 16 – Start routing of each net starting with timestamp = 0 for each net. It is also assumed that transition time for a droplet between two adjacent cells to be of One unit.Compute the arrival time for each droplet – mark the maximum of all arrival times as the latest arrival time T. If T = max (D_i) – it is possible to conclude that route is optimized- because max (D_i) represents the critical path among all the nets. Finally count the total number of cells utilized – E and the number of cells sharing multiple droplets representing total number of contaminations C.

Output: The final layout representing optimized route paths .the overall route time, the latest arrival time and the average arrival time (overall route time/number of droplets) ,the total number of contaminations remaining and number of cells utilized.

VI. AN ILLUSTRATIVE EXAMPLE

The implementation of the algorithm is demonstrated using an illustrative example as shown in figure 4. In figure 4 a) a given layout has been displayed .The layout is comprised of 4 Two pin and One Three pin net with Two hard blockages namely M1 and M2.The paths for each droplet with corresponding alternatives are displayed as Pni where n = a,b,c,d or e (droplet name) and i indicates the corresponding path number for the said droplet.For Three pin droplet path name is indicated by Pnxi and Pnyi for sources n_x and n_y to the mixer respectively.The path Pnti represents the path from mixer to the respective target.Figure 4 b) displays the droplet intersection graph together with linkages to the hard blockages or modules indicating paths for the said net passes through the module.The weightage to the edges represents the number of paths for the nets are involved in the cross over.Figure 4 c) shows the initial path intersection graph .The vertices with scar marks are marked for deletion with corresponding incident edges shown by patterned green line. The grey colored edge represents allowable crossover or contamination as evident for the same members of a three pin net.The red colored edges connecting the paths with modules represent paths that crosses over the said modules.Figure 4 d) shows the final path intersection graph after iterative selection of suitable paths. Figure 4 e) represents the resulting layout with currently selected paths after omission of the redundant ones.Figure 4 f) represents the additional paths introduced after deviation to bypass the hard blockages .In figure 4 g) the path intersection graph is redrawn – where the four friction zones are indicated by hyperpath 1, hyperpath 2 , hyperpath 3 and hyperpath 4. The path with available alternative is omitted to elliminate the friction zones avoiding possible stalling. Moreover other paths have been preferably selected using the technique mentioned in Step 6 in section V.The final layout with route paths and corresponding route results are shown in figure 4 h). However the remaining friction zones formed in the layout are found to be free of stalling – as droplets clears of without any violation of fluidic constraints. The latest arrival time is found to be 12 , average arrival time is 10.4 ,cell utilization being - 51.the number of unavoidable contaminations are limited to 3(indicated by pink cells) with allowable contamination being 1(indicated by green cell).

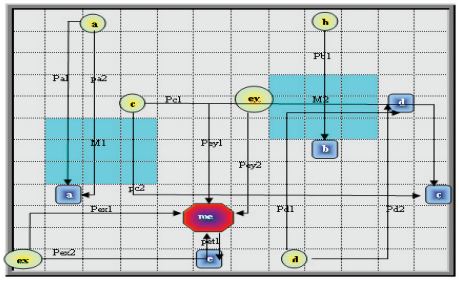

Figure 4 a) initial layout with 4 two pin and 1 Three pin net –and two modules M1 and M2 .All estimated route paths with redundant alterna -tives are shown.

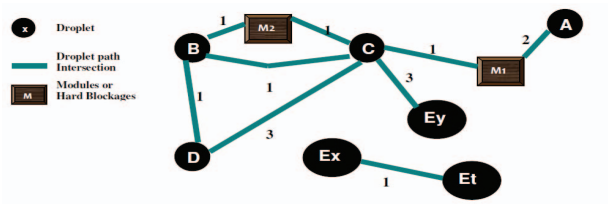

Figure 4 b) the droplet intersection graph with module linkages by paths are shown

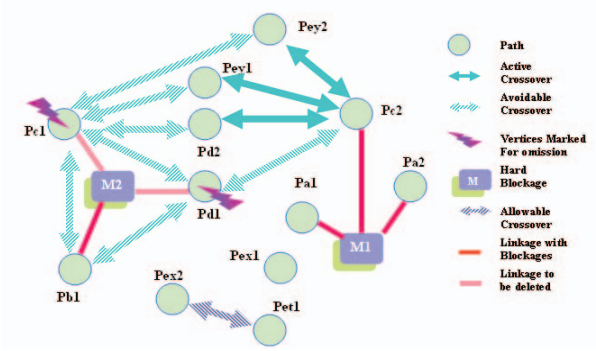

Figure 4 c). Initial path intersection graph indicating redundant paths and crossover determined for omission.

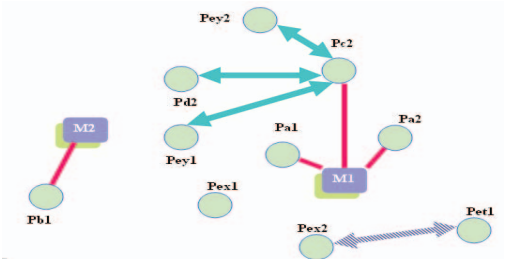

Figure 4 d). Final path intersection graph after iterative selection of the suitable paths.

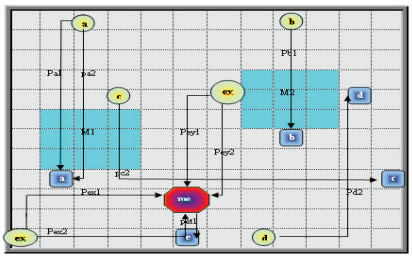

Figure 4 e). the resulting layout with currently selected paths after omission of the redundant ones.

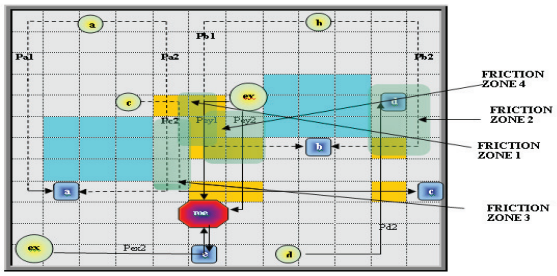

Figure 4 f). layout with the additional paths being introduced after deviation to bypass the hard blockages indicating the friction zones.

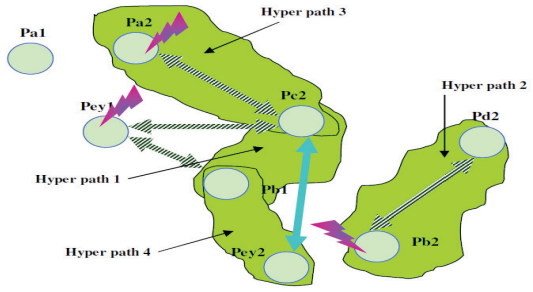

Figure 4 g). the new path intersection graph– where the four friction zones are indicated by hyperpath 1, hyperpath 2 , hyperpath 3 and hyperpath 4.

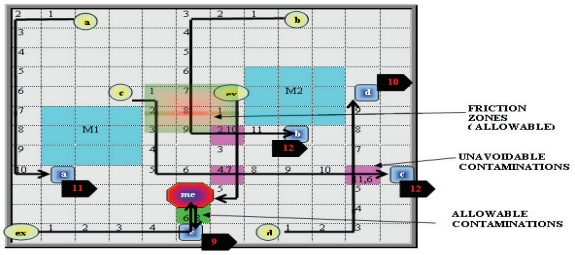

Figure 4 h). The final layout with route paths and corresponding route results.

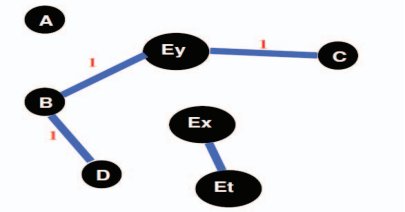

Figure 4 i) Final droplet intersection graph showing Four edges with Three unavoidable and One allowable contamination

VII. EXPERIMENTAL RESULTS

The proposed technique for exploration of suitable route path with an objective of minimizing number of contaminations as well as enhancing the routing performance has been applied on Testbenches of Benchmark suite I and III.The detailed routing result both with and without cross contamination for 11 subproblems of testbench In_vitro 1 in benchmark suite III has been displayed in Table 1. Table 2 displays summarized results for testbenches In_Vitro 1,In_Vitro 2,protein 1 and protein 2 of Benchmark suite III. The results for few testbenches of benchmark suite I have been given in Table 2. Finally in Table 4 few comparative results with performances of contemporary methods is displayed to establish the effectiveness of the proposed technique.

It has been found that in most cases for benchmark suite III cell utilization has been increased but Maximum arrival time as well as average arrival time increased in some cases only marginally. This implies that as more detours are necessary to avoid cross contamination that contributes towards increase in cell utilization on the other hand Route time has been kept to be optimum that results in only marginal increase in certain cases of the average arrival time with almost no variation in maximum arrival time. The contaminations are found to be reduced considerably in almost all the cases.

However for testbenches in benchmark suite I as number of droplets are more in comparison to grid size – little space are available to provide alternate path or necessary detour to avoid contamination. Still the proposed method has attempted to reduce number of contamination with optimized route performance.

Table 1: detailed route performance for test bench In Vitro 1

Sub Problem [Grid] 16 x 16	Droplet Type		Results With Cross Contamination				Results With optimized Cross Contamination			
	2 Pin	3 Pin	Latest Arrival Time	Avg. Arrival Time	Cells Used	Contm -ination	Latest Arrival Time	Avg. Arrival Time	Cells Used	Contam -ination
1	2	1	20	17.67	41	10	22	18.6	56	2
2	2	1	25	14.67	48	0	25	14.67	48	0
3	3	2	20	13.8	56	10	22	13.4	66	2
4	1	0	5	5	5	0	5	5	5	0
5	0	2	21	20.5	29	0	21	20.5	29	0
6	4	0	10	8.75	32	0	10	8.75	32	0
7	2	0	10	9	14	4	10	9	18	0
8	2	0	9	7.5	15	0	9	7.5	15	0
9	2	0	10	8	16	0	10	8	16	0
10	1	0	9	9	9	0	9	9	9	0
11	1	0	10	10	10	0	10	10	10	0
Total	20	6	149	123.9	275	24	153	124.4	304	4 Reduction (83.33%)
Average Value			13.54	11.26	25		13.9	11.31	27.63	
Maximum Value			25	20.5	56	10	25	20.5	66	2

VIII. CONCLUSION

In this work we proposed a specific technique that performs intelligent exploration of cross contamination aware virtual route paths that not only minimizes the overall number of contaminations but also the overall route time together with latest arrival time for all the droplets involved in the execution of the specified protocol.It has been found so far that on implementation of the proposed algorithm – an encouraging improvement has been achieved in comparison to contemporary methods. In this paper we have employed a graph based heuristic to identify suitable alternatives for intelligent avoidance of cross contaminations while maintaining optimum route performance in digital microfluidic Biochips. But there still remain scopes for further improvement using finer adjustment of the nets using meticulous placement and compaction techniques.

Table 2: Cross contamination aware route results for benchmark suite III

Test bench	Grid Size	With cross contamination				Without cross contamination				Reduction (%)
		Max Arrival Time	Average Arrival Time	Cells Used	Contamination	Max Arrival Time	Average Arrival Time	Cells Used	Contamination	
In Vitro1	16 x 16	19	11.26	275	24	19	11.31	304	4	83.33%
In Vitro2	14 x 14	19	8.923	246	11	20	8.856	270	4	63.60%
Protein 1	21 x 21	20	11.165	1786	114	20	10.98	1847	22	80.71%
Protein 2	13 x 13	18	6.88	1097	75	18	7.04	1174	18	76.00%

Table 3: Cross contamination aware route results for selected test benches in benchmark suite I

Test bench	Grid Size (droplets)	With cross contamination				Without cross contamination				Reduction (%)
		Max Arrival Time	Average Arrival Time	Cells Used	Contamination	Max Arrival Time	Average Arrival Time	Cells Used	Contamination	
Test 12_12_1	12 x 12 (12)	24	13.67	65	66	24	11.91	76	53	19.69%
Test 12_12_2	12 x 12 (12)	19	11.42	61	70	20	6.16	78	51	27.14%
Test 12_12_3	12 x 12 (12)	21	11.17	70	89	23	14.58	69	71	20.23%
Test 16_16_1	16 x 16 (16)	30	15.75	117	110	30	12.0	133	96	12.72%
Test 16_16_2	16 x 16 (16)	25	14.4	113	110	23	6.8	130	83	24.54%
Test 16_16_3	16 x 16 (16)	34	15.437	116	148	30	9.1	143	114	22.97%
Test 16_16_4	16 x 16 (16)	31	14.73	114	115	31	11.6	125	84	26.95%
Test 24_24_1	24 x 24 (24)	35	23.25	249	298	45	21.375	293	267	10.40%
Test 24_24_2	24 x 24 (24)	43	20.17	251	269	46	11.79	301	196	27.14%

Table 4: comparison of Cross contamination aware route results with contemporary methods for Benchmark suite III.

Test bench	Zhao and Chakrabarty [25]				Huang,Lin,Ho [15]				Our Method			
	Cntm	C.U	T_{EX}	CPU	Cntm	C.U	T_{EX}	CPU	Cntm	C.U	T_{EX}	CPU
In Vitro1	4	621	268	0.06	21	351	193	0.58	4	304	149	0.25
In Vitro2	0	423	224	0.03	5	281	191	0.39	3	270	172	0.20
Protein 1	18	3215	1508	0.23	82	2213	1394	2.58	22	1847	1012	1.05
Protein 2	11	1574	1287	0.14	61	1362	1108	1.49	18	1174	755	0.55
Total	33	5833	3287	0.46	169	4207	2886	5.04	47	3595	2088	2.05

Cntm – Total Number of Contaminations *C.U – Overall cell utilization*
T_{EX} - Total execution time for Test bench *CPU – The CPU time (sec.)*

REFERENCES

[1] M.G. Pollack, R.B. Fair, and A.D. Shenderov, "Electrowetting-based actuation of liquid droplets for microfluidic applications," *Appl.PhysLett* 77 1725- 1727 (2000).

[2] J. Lee, H. Moon J. Fowler, C.-J Kim and T.Schoellhammer, "Addressable micro liquid handling by electric control of surface tension," Proc. of 2001 IEEE 14th International Conference on MEMS, Interlaken,Switzerland 499-502 (2001).

[3].R.C.Gascoyne, and J.V Vykoukal,"Dielectrophoresis based sample handling in general-purpose programmable diagnostic Instruments," *Proc. IEEE* 92 .22-42 (2004).

[4]D.A. Anton, J.P. Valentino, S.M. Trojan, and S Wagner,"Thermocapillary actuation of droplets on chemically patterned surfaces by programmable microheater arrays," *J Microelectromechanical Sys.* 12 .873-879 (2003)

[5]A. Renaudin, P. Tabourier , V. Zhang, C. Druhon and J.C. Camart "Plateforme SAW dédiée à la microfluidique discrète pour applications biologiques", 2ème Congrès Français de Microfluidique,Société Hydrotechnique de France, Toulouse, France, 14-16 (2004).

[6] S.K. Cho, H. Moon, and C.J. Kim, "Creating, transporting, cutting, and merging liquid droplets by electrowettingbased actuation for digital micro fluidic circuits," *Journal of Microelectromechanical Systems*, vol. 12, 2003, pp. 70-80.

[7] Alborz Arzpeyma, Shan Bhaseen, Ali Dolatabadi, Paula Wood-Adams, "A coupled electro-hydrodynamic numerical modeling of droplet actuation by electrowetting," Colloids and Surfaces A: Physicochem. Eng. Aspects, vol. 323, pp. 28-35,2008.

[8] Y-H Chang, G-B Lee, F-C Huang, Y-Y Chen, J-L Lin, "Integrated polymerase chain reaction chips utilizing digital microfluidics," Biomed Microdevices , vol. 8, pp. 2 15-225, 2006.

[9] V Srinivasan, VK Pamula, RB Fair, "An integrated digital microfluidic lab-on-a-chip for clinical diagnostics on human physiological fluids,"Lab Chip, vol. 4, pp. 310-315, 2004.

[10] H Moon, AR Wheeler, RL Garrell, JA Loo, CJ Kim, "An integrated digital microfluidic chip for multiplexed proteomic sample preparation and analysis," by MALDI-MS. Lab Chip, vol. 6, pp. 1213-1219, 2006.

[11] M Abdelgawad, Aaron R. Wheeler, "Low-cost, rapid-prototyping of digital microfluidics devices," Microfluid Nanofluid, vol. 4, pp. 349-355, 2007.

[12] J. Berthier, Microdropes and Digital Microfluidics, William Andrew Inc,Norwich, NY, 2008.

[13] F Su, Jun Zeng," Computer aided design and test for digital microfluidics ",*IEEE* Design and test for computers, pp. 60-70. Feb, 2007.

[14]T.-Y. Ho, J. Zeng, and K. Chakrabarty, "Digital microuidic biochips: A vision for functional diversity and more than Moore," Proc. ACM/IEEE ICCAD, pp. 578{585, 2010.

[15] Tsung-Wei Huang, Chun-Hsien Lin, and Tsung-Yi Ho,"A contamination aware droplet routing algorithm for digital microfluidic biochips ", *ICCAD'09,* November 2–5, 2009, San Jose, California, USA.

[16] Akella S., Griffith E. J. and Goldberg. M. K. "Performance character -- ization of a reconfigurable planar-array digital microfluidic system", *IEEE Transactions Computer-Aided Design of Integrated Circuits and Systems,* 25(10), pp. 340-352, Feb, 2006.

[17] P. Yuh , S. Sapatnekar, C. Yang, and Y. Chang, "A progressive-ilp based routing algorithm for cross referencing biochips," *Design Automation Conference*, pp. 284–289, 2008.

[18] H. William, Su Fei and Chakrabarty K., "Droplet routing in the synthesis of digital microfluidic biochips." In Proc. *of Design Automation & Test in Europe*, 2006.

[19] Cho Minsik and Pan. David Z. "A high-performance droplet routing algorithm for digital microfluidic biochips." *IEEE Transactions Computer Aided Design of Integrated Circuits and Systems*, 27(10), pp. 406-419, 2008.

[20]T. Xu and K. Chakrabarty." Droplet-trace-based array partitioning and a pin assignment algorithm for the automated design of digital microfluidic biochips." In *CODES+ISSS*, pp. 112–117, Oct. 2007.

[21] Tsung-Wei Huang, Tsung-Yi Ho, "A Fast Routability and Performance-driven droplet routing algorithm for digital microfluidic biochips"- *Computer Design, 2009. ICCD 2009. IEEE International Conference 4-7, Oct.2009,* pp. 445-450 Lake Tahoe, CA.

[22] Soukup J, "Fast Maze Router" *Proceedings of the 15th ACM Design Automation Conference,* pp. 100 102, 1978.

[23] P Roy, H Rahaman, P Dasgupta, "A Novel Droplet Routing Algorithm for Digital Microfluidic Biochips", *Proc. of the* GLSVLSI, 2010, Providance, Rhode Island, USA.

[24] Zigang Xiao, Evangeline F. Y. Young," Droplet Routing Aware Module Placement for CrosReferencing Biochips",*ISPD2010*, San Fransisco California, USA,17th March,2010.

[25] Yang Zhao and Krishnendu Chakrabarty,"Synchronization of Washing Operations with Droplet Routing for Cross-Contamination Avoidance in Digital Microfluidic Biochips"*Proc. Of DAC'10*, June 13-18, 2010, Anaheim, California, USA.

[26] T.-W. Huang and T.-Y. Ho, "A Two-Stage ILP-Based Droplet Routing Algorithm for Pin-Constrained Digital Microuidic Biochips" Pro. of ACM ISPD, Mar. 2010.

[27] Yang C.L, Yuh P.H. and Chang. Y.W. "Bioroute: A network flow based routing algorithm for digital micro fluidic biochips." In *Proceedings of IEEE/ACM International Conference on ComputerAided Design*, pages 752-757, 2007.

[28] P. Roy, H. Rahaman , R. Bhattacharya, P.S. Dasgupta "A Best Path Selection Based Parallel Router For DMFBs"*Proc. of ISED 2011,IEEE International Conference,*pp. 176-181, December,2011,Kochi,India

[29] Y. Zhao and K. Chakrabarty, "Cross-contamination avoidance for droplet routing in digital microfluidic biochips,"*IEEE/ACM DATE*, Apr. 2009.